Acta Cryst. (1996). D52, 882–886

Crystalline alcohol dehydrogenases from the mesophilic bacterium *Clostridium beijerinckii* and the thermophilic bacterium *Thermoanaerobium brockii*: preparation, characterization and molecular symmetry

YAKOV KORKHIN,[a] FELIX FROLOW,[b] OREN BOGIN,[c] MOSHE PERETZ,[c] A. JOSEPH KALB (GILBOA)[a] AND YIGAL BURSTEIN[c] *at Departments of [a]Structural Biology, [b]Chemical Services and [c]Organic Chemistry, The Weizmann Institute of Science, Rehovot 76100, Israel. E-mail: cvfrolow@wicc.weizmann.ac.il*

(Received 3 January 1996; accepted 31 January 1996)

Abstract

Two tetrameric $NADP^+$-dependent bacterial secondary alcohol dehydrogenases have been crystallized in the apo- and the holo-enzyme forms. Crystals of the holo-enzyme from the mesophilic *Clostridium beijerinckii* (NCBAD) belong to space group $P2_12_12_1$ with unit-cell dimensions $a = 90.5$, $b = 127.9$, $c = 151.4$ Å. Crystals of the apo-enzyme (CBAD) belong to the same space group with unit-cell dimensions $a = 80.4$, $b = 102.3$, $c = 193.5$ Å. Crystals of the holo-enzyme from the thermophilic *Thermoanaerobium brockii* (NTBAD) belong to space group $P6_{1(5)}$ ($a = b = 80.6$, $c = 400.7$ Å). Crystals of the apo-form of TBAD (point mutant G198D) belong to space group $P2_1$ with cell dimensions $a = 123.0$, $b = 84.8$, $c = 160.4$ Å $\beta = 99.5°$. Crystals of CBAD, NCBAD and NTBAD contain one tetramer per asymmetric unit. They diffract to 2.0 Å resolution at liquid nitrogen temperature. Crystals of TBAD(G198D) have two tetramers per asymmetric unit and diffract to 2.7 Å at 276 K. Self-rotation analysis shows that both enzymes are tetramers of 222 symmetry.

1. Introduction

The stability of proteins under extreme conditions of temperature, ionic strength, pH, *etc.* is a problem which has always intrigued biochemists. To understand the underlying principles, it is of great importance to compare the three-dimensional structures of proteins sharing high sequence identity but differing in their degree of tolerance to harsh environments. For this purpose, the alcohol dehydrogenases from the mesophilic *Clostridium beijerinckii* (Ismael, Zhu, Colby & Chen, 1993) and the thermophilic *Thermoanaerobium brockii* (Peretz & Burstein, 1989) have been isolated and purified. These enzymes belong to the family of medium-chain zinc-containing tetrameric alcohol dehydrogenases and have 75% sequence identity and 88% sequence homology (Reid & Fewson, 1994). They differ, however, in their thermal stability (Bogin, Peretz & Burstein, 1995) and in their resistance to denaturing agents. The extent of resistance to denaturation of TBAD depends on the presence of the cofactor (Burstein, unpublished results). Primary structure and purification to homogeneity of CBAD (351 amino-acid residues per monomer) and TBAD (352 amino-acid residues per monomer) have been reported (Rifaat & Chen, 1992; Peretz & Burstein, 1989). Both enzymes share only 27% sequence identity with horse liver alcohol dehydrogenase (HLADH) (Eklund *et al.*, 1976) and human alcohol dehydrogenase (HADH) (Hurley, Bosron, Hamilton & Amzel, 1991) the only proteins of the medium-chain Zn-containing family whose X-ray structures have been solved. The X-ray structure of a tetrameric glucose dehydrogenase (GDH) from the thermophilic archaeon *Thermoplasma acidophilum*, having approximately 19% sequence identity with CBAD or TBAD, has been reported (John, Crennell, Hough, Danson & Taylor, 1994).

Two crystal forms of TBAD have been reported earlier (Zhang *et al.*, 1993). Here we describe new crystal forms of TBAD and of its mutant G198D as well as the first crystallization of CBAD as the holo-enzyme and in its NADP (nicotinamide–adenine dinucleotide phosphate)-free form.

2. Materials and methods

2.1. *CBAD*

The protein was overexpressed in *Escherichia coli* and purified to homogeneity (Bogin *et al.*, 1995). Crystals (Fig. 1*a*) were grown from hanging drops at 293 K. 3 µl of protein stock solution [15 mg ml^{-1} of protein, 50 m*M* Tris–HCl, 50 m*M* NaCl, 0.1 m*M* DTT (dithiothreitol), 50 µ*M* $ZnCl_2$, pH = 7.3] was mixed with 3 µl of reservoir solution (16% PEG 4000, 50 m*M* NaCl, 50 m*M* Tris–HCl, pH = 7.5). Crystals appeared after 2 d and developed to a final size of about 0.5 × 0.3 × 0.3 mm over a period of 7–10 d. For data collection under cryogenic conditions crystals were transferred through a series of harvesting solutions in which the concentration of ethylene glycol was doubled in six steps starting from 0.5%(*v*/*v*) to a final concentration of 15%(*v*/*v*). Crystals were kept in each solution for 20 min. Crystals were mounted in loops made of fine surgical thread and flash frozen in liquid nitrogen. Data were collected at beamline X12C of the National Synchrotron Light Source (NSLS) at the Brookhaven National Laboratory (see Table 1 for details). The crystals diffracted to at least 2.0 Å resolution with a mosaic spread of 0.15°.

2.2. *NCBAD*

Conditions for NCBAD crystallization were assessed on the basis of two-dimensional phase diagram for protein concentration *versus* PEG concentration using the IMPAX small-volume automated crystallization system and microbatch crystallization under oil (Chayen, Shaw Stewart, Maeder & Blow, 1990) (Chayen, Shaw Stewart & Baldock, 1994). Crystals (Fig. 1*b*) were grown in 8 µl sitting drops containing 6.5 mg ml^{-1} of enzyme, 1.5 m*M* $NADP^+$, 10.5% PEG 4000, 50 m*M* NaCl, 50 m*M* Tris–HCl, pH 8.2 seeded with 0.3 µl of a 1/10000 dilution of a finely crushed microcrystalline suspension and equilibrated against a 100 µl reservoir containing salts as above and 11.5% PEG 4000. Crystals appeared after 4–5 d and reached a maximum size of about 0.5 × 0.5 × 0.3 mm within the next 10–14 d. For data collection under cryogenic conditions the stepwise transfer into cryoprotectant and flash freezing

Table 1. *Properties of four bacterial alcohol dehydrogenase crystals*

	CBAD	NCBAD	NTBAD	G198D
Space group	$P2_12_12_1$	$P2_12_12_1$	$P6_{1(5)}$	$P2_1$
Cell dimensions (Å,°)	$a = 80.4$, $b = 102.3$, $c = 193.5$	$a = 90.5$, $b = 151.4$, $c = 127.9$	$a = b = 80.6$, $c = 400.7$	$a = 123.0$, $b = 84.8$, $c = 160.4$, $\beta = 99.5$
Subunits/ asymmetric unit	4	4	4	8
V_M (Å^3 Da^{-1})	2.67	2.94	2.52	2.77
Data collected*	B	B	F	H
Highest resolution observed (Å)	2.0	2.0	2.0	2.7

* B = beamline X12C, NSLS, Brookhaven National Laboratory. The wavelength (1.25 Å) was optimized for the anomalous signal from the intrinsic Zn. F = beamline BL-6A, Photon Factory, KEK. Data were collected on imaging plates with a Weissenberg camera of radius 430 mm. Wavelength was 1.0 Å. H = data were collected with a Xentronics area detector using Cu $K\alpha$ radiation.

used for CBAD crystals was successful. Data were collected at beamline X12C of NSLS (Table 1). The crystals diffracted to at least 2.0 Å resolution with a mosaic spread of 0.20°.

2.3. *NTBAD*

Crystallization of TBAD has been reported (Zhang *et al.*, 1993) in several crystal forms which were, however, highly sensitive to radiation damage. As in the case of NCBAD described above, we used a phase diagram of protein *versus* precipitant to guide us to optimal conditions. A new crystal form (Fig. 1*c*), stable to radiation, grew in 8 µl sitting drops (6.8 mg ml^{-1} of protein, 2 m*M* NADP$^+$, 50 m*M* Tris–HCl, 50 m*M* NaCl, 0.1 m*M* DTT, 50 µ*M* $ZnCl_2$, 14% PEG 4000, pH = 8.3) seeded with 0.3 µl of a dilute suspension of crushed microcrystals equilibrated against a 100 µl reservoir (15.5% PEG 4000, 50 m*M* NaCl, 50 m*M* Tris–HCl pH = 8.3). Crystals appeared after 4–6 d and grew to a maximum size of about 0.8 × 0.8 × 0.3 mm in the course of the next 2–3 weeks. We characterized these crystals at room temperature with a Xentronics area detector on a Rigaku RU-300 rotating-anode generator equipped with Charles Supper double-focusing mirrors and a helium path. Crystals were stable in the beam, diffracted to at least 2.5 Å resolution and had extremely sharp diffraction (mosaicity 0.1°). Several cryoprotectants were tried, including MPD (2-methyl-2,4-pentanediol), PEG 400, glycerol and ethylene glycol. The best results were obtained with 15% ethylene glycol or 15% glycerol in conjunction with the gradual transfer procedure described above and flash freezing in liquid propane. Upon freezing, the mosaicity increased to 0.3° which, together with the 400 Å length of the *c* axis, makes high-resolution data collection under cryogenic conditions problematic. Frozen crystals diffract to 2.0 Å resolution with synchrotron radiation. The best data set, however, was collected to 2.5 Å resolution at room temperature at beamline BL-6A at the Photon Factory (Table 1).

2.4. *G198D*

Attempts to define reproducible conditions for growing crystals of the apo-form of the wild-type TBAD and of several point mutants (C203S, C203K) were unsuccessful. The best apo-form crystals (Fig. 1*d*), however, were obtained with the TBAD point mutant G198D (Peretz *et al.*, 1995) at 277 K by hanging-drop vapor diffusion: 3 µl of protein stock solution (58 mg ml^{-1} of protein, 20 m*M* KCl) was mixed with an equal volume of solution containing 12% PEG 4000, 0.4 *M* KCl, 50 m*M* Tris–HCl (pH = 8.5) and equilibrated over a 1 ml reservoir containing 15% PEG 4000, 0.4 *M* KCl, 50 m*M* Tris–HCl, pH = 8.5. Crystals developed in the course of 3–7 d and reached a final size of about 1 mm in the largest dimension. Data were collected with a Xentronics area detector and a Rigaku RU-300 rotating-anode generator operating at 10 kW equipped with a graphite monochromator and a long, evacuated collimator. The crystals were sensitive to temperature variations. Therefore, all crystal handling was performed in a cold room (277 K) and the crystals were maintained at exactly 276 (0.2) K during data collection with the aid of a heat-exchange-type cryostat (Oxford Cryostream). The crystals diffracted to 2.7 Å resolution and had a mosaic spread of 0.3°. See Table 1 for details.

2.5. *Determination of crystallographic parameters*

Data were processed with the data-processing packages *DENZO-SCALEPACK* (Otwinowski & Minor, 1996) or *XDS-XSCALE* (Kabsch, 1988).

2.6. *Self-rotation analysis*

Rotation functions were calculated by means of the general and locked rotation function (Tong & Rossmann, 1990) as implemented in the molecular-replacement package *REPLACE* (Tong, 1993).

3. Results

Properties of the four crystal forms are summarized in Table 1.

3.1. *Molecular symmetry*

3.1.1. *CBAD.* One asymmetric unit of the $\kappa = 180°$ section of the self-rotation stereogram is presented in Fig. 2(*a*). One non-crystallographic twofold axis ($\varphi = 90$, $\psi = 45°$) can be clearly identified, as well as two smaller peaks ($\varphi = 52$, $\psi = 52$ and $\varphi = 22$, $\psi = 70°$). A significant peak at $\varphi = 0$, $\psi = 90°$ was identified on the $\kappa = 90°$ section of the map, which could mean a possible non-crystallographic fourfold axis parallel to the crystallographic *b* axis. This interpretation is, however, inconsistent with the absence of any significant peaks on the $V = 1/2$ Harker section of Patterson map even at low resolution (40–12 Å). A more likely interpretation is that the peak is a product of group multiplication between crystallographic and non-crystallographic twofold axes following one another every 45° in the *UW* plane in Patterson space. The two smaller peaks on the $\kappa = 180°$ section do, indeed, correspond to the expected peaks for two of the twofold axes required by 222 point-group symmetry. This is confirmed by superimposing the $\varphi = 90$, $\psi = 45°$ directions in the rotated and the non-rotated cells and calculating a one-dimensional self-rotation function. Two outstanding peaks at 90° intervals were clearly identified whose angular values corresponded to the two suspected peak positions. The three peaks at $\varphi = 90$, $\psi = 45°$; $\varphi = 52$, $\psi = 52°$

and $\varphi = 22$, $\psi = 70°$ thus form a set of true non-crystallographic twofold axes of a 222 tetramer.

3.1.2. *NCBAD.* The asymmetric unit of the $\kappa = 180°$ section of the self-rotation function map is presented in Fig. 2(*b*). The three peaks ($\varphi = 58$, $\psi = 80°$; $\varphi = 56$, $\psi = 24°$; $\varphi = 28$, $\psi = 68°$) forming a set of twofold axes of the 222 tetramer can be clearly identified.

3.1.3. *NTBAD.* The $\kappa = 180°$ section of the self-rotation function map is presented in Fig. 2(*c*). A major non-crystallographic twofold axis is observed every 30° in the $\varphi = 0°$ equatorial plane, creating a *pseudo* 622 pattern. If each of the equatorial peaks represents a true non-crystallographic twofold axis, then the third twofold axis must be parallel to the unique crystallographic axis. But again no significant peaks were identified on the $W = 1/2$ Harker section of the Patterson map. Thus, only one peak represents a true non-crystallographic rotation symmetry and the second one is generated by combination of crystallographic and non-crystallographic symmetry. To find out which of the two equatorial axes was a true non-crystallographic twofold axis and the positions of the other two axes of the 222 symmetry of the tetramer we performed two one-dimensional self-rotation function calculations at $\varphi = 90$, $\kappa = 180°$ and at $\psi = 90$, $\kappa = 180°$. No peaks were found for the first orientation, however, two peaks at $\varphi = 28.5°$ and at $\varphi = 118.5°$ were identified for the second orientation. Hence, the three mutually perpendicular twofold axes constituting the 222 non-crystallographic symmetry in this crystal form are at $\varphi = 0$, $\psi = 0°$; $\varphi = 28.5$, $\psi = 90°$ and $\varphi = 118.5$, $\psi = 90°$.

3.1.4. *G198D–TBAD.* The $\kappa = 180°$ section of the self-rotation stereogram is presented in Fig. 2(*d*). Three peaks at ($\varphi = 172$, $\psi = 56°$; $\varphi = 98$, $\psi = 66°$; $\varphi = 36$, $\psi = 42°$) forming a set of twofold axes of the 222 tetramer can be clearly identified. The data show systematically weak intensities for reflections with $l = 2n + 1$ and the Patterson map has a prominent peak at (0.0, 0.0, 0.5) equal in height to the origin peak, which suggests that there is a near 1/2 translation along the crystallographic *c* axis between the two tetramers in the asymmetric unit.

4. Discussion

Attempts to solve the three-dimensional structures of these enzymes by molecular replacement using the structures of HLADH and GDH as models are under way. Although sequence homology is low, we may expect a high degree of structural homology, especially in the regions of the Rossmann fold, the cofactor binding site and the active site (Reid &

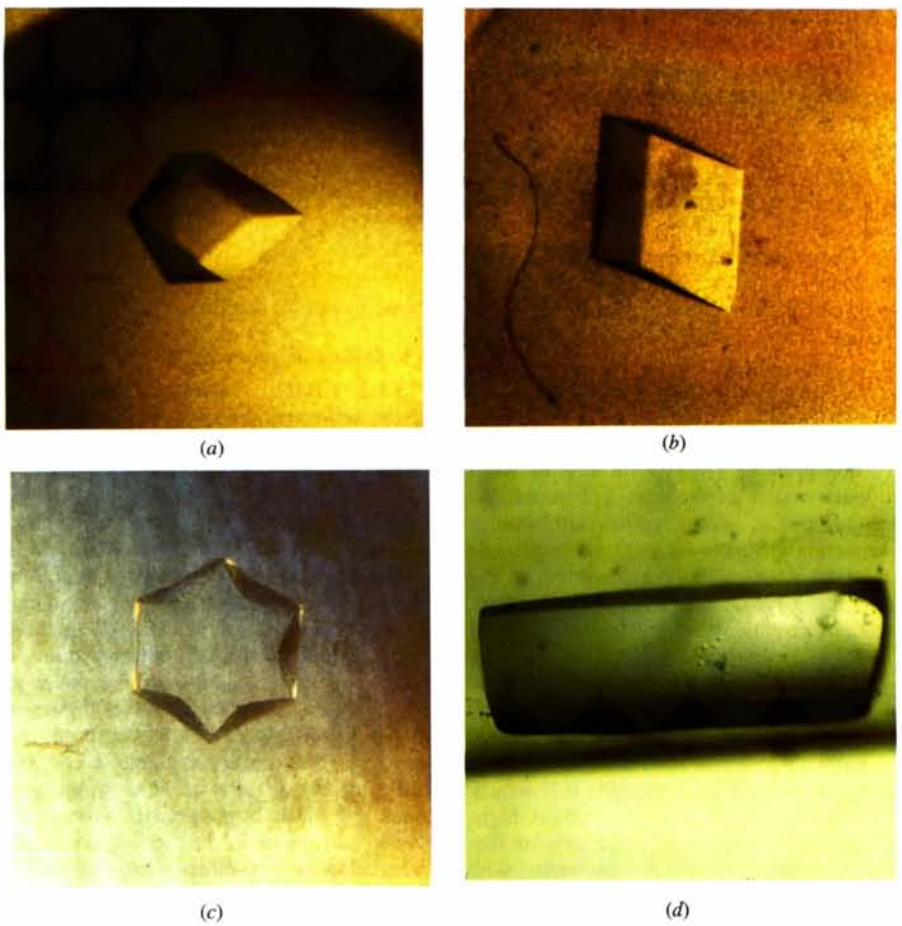

(*a*) (*b*) (*c*) (*d*)

Fig. 1. Photomicrographs of crystalline alcohol dehydrogenases for (*a*) CBAD; (*b*) NCBAD; (*c*) NTBAD and (*d*) TBAD (G198D).

Fewson, 1994). Once an appropriate model is correctly positioned in the cell non-crystallographic symmetry that we have reported here will be useful for phase determination by the poweful methods of symmetry averaging and solvent flattening (Rossmann, 1990; Rossmann *et al.*, 1992).

A search for heavy-atom derivatives is in progress. There are five cysteinyl residues in CBAD and four in TBAD. Cys37 is involved in Zn-atom coordination, Cys283 and Cys295 are not susceptible to alkylation, which leaves Cys85 and Cys203 in CBAD and Cys203 in TBAD as possible targets for preparation of mercurial derivatives. Cys203 of apo-TBAD but not of the holo-enzyme can be modified in solution by mercurials (Burstein, unpublished results).

A Patterson cross-rotation function between the data sets for CBAD and TBAD has been calculated yielding outstanding peaks. This suggests a high degree of structural homology.

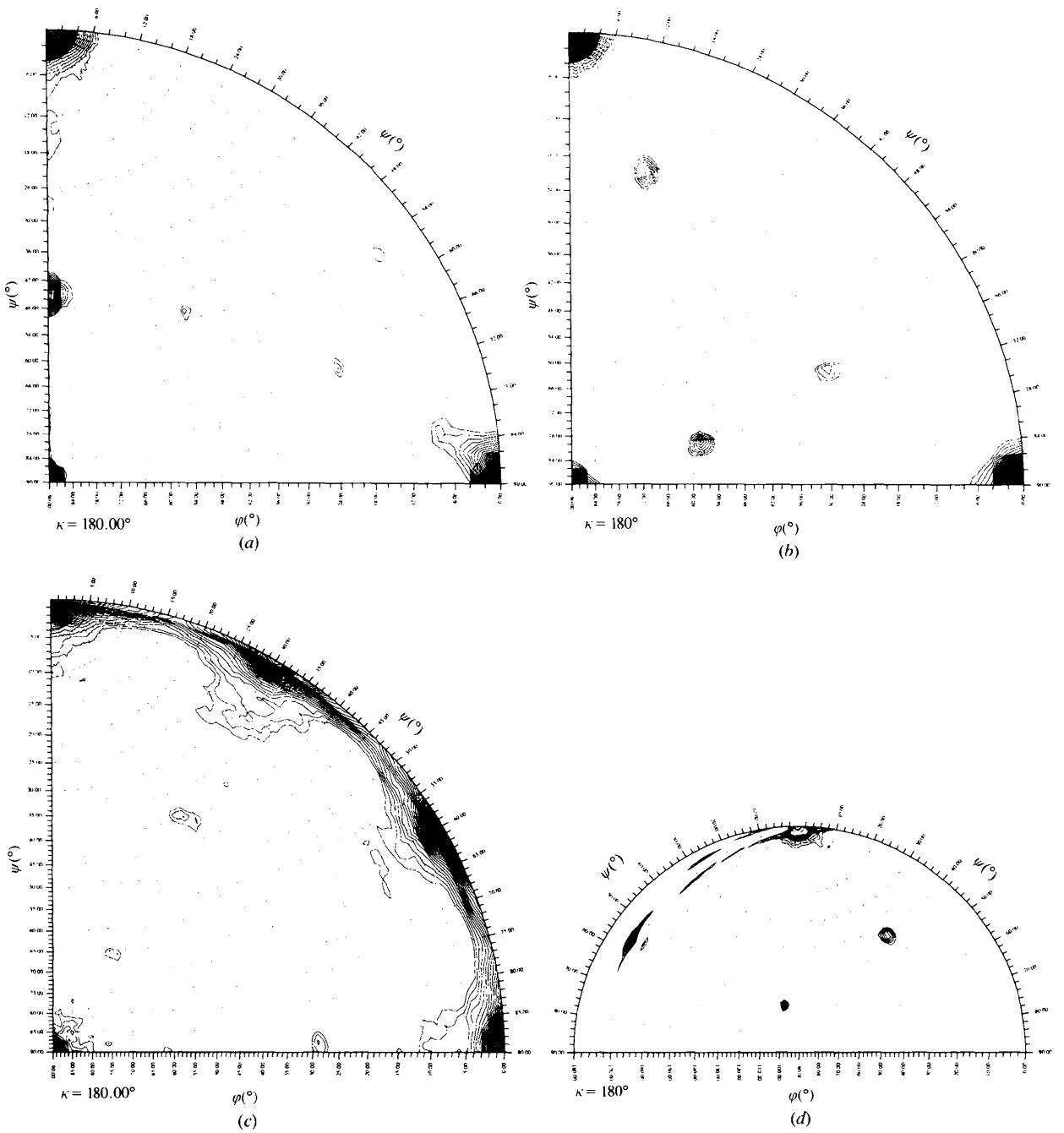

Fig. 2. $\kappa = 180°$ sections of self-rotation maps for (*a*) CBAD; (*b*) NCBAD; (*c*) NTBAD and (*d*) TBAD (G198D).

Thus, once one of these structures is solved the other should be easily solved by molecular replacement by using the first one as a model. Comparison of the crystal structures of these highly homologous enzymes and of the holo-enzymes with their apo-forms will provide detailed information to address the issues of protein thermostability.

We thank the support staff of the beamlines X12C at the National Synchrotron Light Source, BNL, and BL6A at the Photon Factory, KEK for their assistance in using the equipment of the stations.

Note added in proof: the structure of CBAD has been solved by isomorphous replacement and anomalous scattering from a single mercurial derivative and refined to a resolution of 2.8 Å (PDB entry 1PED). The strucutre of NTBAD has been solved by molecular replacement based on the above coordinates and refined to resolution of 2.5 Å (PDB entry 1YKF). The structures of NCBAD and G198D-TBAD have been solved by molecular replacement and their refinement is in progress.

References

Bogin, O., Peretz, M. & Burstein, Y. (1995). Abstracts of The First Meeting of Federation of the Israeli Societies of Experimental Biology, Eilat, October 17–20, p. 58.

Chayen, N. E., Shaw Stewart, P. D. & Baldock, P. (1994). *Acta Cryst.* D**50**, 456–458.

Chayen, N. E., Shaw Stewart, P. D., Maeder, D. L. & Blow, D. M. (1990). *J. Appl. Cryst.* **23**, 297–302.

Eklund, H., Nordstrom, B., Zeppezauer, E., Soderlund, G., Ohlsson, I., Boiwe, T., Soderberg, B.-O., Tapia, O. & Brändén, C.-I. (1976). *J. Mol. Biol.* **102**, 27–59.

Hurley, T. D., Bosron, W. F., Hamilton, J. A. & Amzel, L. M. (1991). *Proc. Natl Acad. Sci. USA*, **88**, 8149–8153.

Ismael, A. A., Zhu, C.-X., Colby, G. D. & Chen, J.-S. (1993). *J. Bacteriol.* **175**, 5097–5105.

John, J., Crennell, S. J., Hough, D. W., Danson, M. J. & Taylor, G. L. (1994). *Structure*, **2**, 385–393.

Kabsch, W. (1988). *J. Appl. Cryst.* **21**, 916–924.

Otwinowski, Z. & Minor, W. (1996). *The HKL Program Suite*. In preparation.

Peretz, M. & Burstein, Y. (1989). *Biochemistry*, **28**, 6549–6555.

Peretz, M., Frankel, Z. B., Meijler, M., Tel-Or, S., Bogin, O. & Burstein, Y. (1995). Abstracts of The First Meeting of Federation of the Israeli Societies of Experimental Biology, Eilat, October 17–20, p. 198.

Reid, M. F. & Fewson, C. A. (1994). *Crit. Rev. Microbiol.* **20**, 13–56.

Rifaat, M. M. & Chen, J.-S. (1992). Unpublished work.

Rossmann, M. G. (1990). *Acta Cryst.* A**46**, 73–82.

Rossmann, M. G., McKenna, R., Tong, L., Xia, D., Dai, J., Wu, H., Choi, H. K. & Lynch, R. E. (1992). *J. Appl. Cryst.* **25**, 166–180.

Tong, L. (1993). *J. Appl. Cryst.* **26**, 748–751.

Tong, L. &. Rossmann, M. (1990). *Acta Cryst.* A**46**, 783–792.

Zhang, Z., Djebli, A., Shoham, M., Frolow, F., Peretz, M. & Burstein, Y. (1993). *J. Mol. Biol.* **230**, 353–355.